7th Int. Symp. "Nanostructures: Physics and Technology"
St Petersburg, Russia, June 14–18, 1999

II–VI laser heterostructures with different types of active region

S. V. Ivanov, A. A. Toropov, T. V. Shubina, S. V. Sorokin, A. V. Lebedev, I. V. Sedova and P. S. Kop'ev
Ioffe Physico-Technical Institute, St Petersburg, Russia

Abstract. We report on the recent development of II–VI room temperature (RT) blue-green lasers based on both (Zn,Mg)(S,Se) and (Be,Mg,Zn)Se material systems, grown by molecular beam epitaxy (MBE). A novel concept of the laser structure design, aimed at enhancement of the degradation stability, is suggested and realized. It involves a combination of alternately-strained short-period superlattice (SL) waveguide (like ZnSSe/ZnCdSe or BeZnSe/ZnCdSe) (for protecting the laser active region from outside penetration of defects) with a single 2–3 ML thick CdSe/ZnSe fractional monolayer (FM) active region transformed under certain MBE conditions into the dense array of 10–50 nm-size CdSe-rich self-organized nanoislands providing effective carrier localization and spatial separation of radiative recombination sites and defects in the active region. As a result, significantly improved optical and electronic confinement as well as high quantum efficiency have been obtained, leading to the lowest ever reported threshold power density ($< 4\,\mathrm{kW/cm^2}$, 300 K) of ZnMgSSe SL FM laser, the highest characteristic temperature ($T_0 = 360$ K at RT) and maximal operational temperature (140°C) of the BeMgZnSe SL QW laser diode. First cw RT laser diodes with the FM active region have been demonstrated. All SL FM lasers have revealed the increased degradation stability with respect to conventional ZnSe-based SCH lasers.

1 Introduction

II–VI wide bandgap heterostructures still remain the only semiconductor system suitable for fabrication of commercial green laser diodes for projection television and other applications requiring the whole set of laser wavelengths in the visible spectral range. Despite the numerous efforts made during the last few years towards optimization of conventional ZnSe-based quantum well (QW) laser diodes, the progress in the lifetime increase is still rather slow [1, 2]. The main origin of the relatively fast laser degradation has been found by Nakano [2] to be non-radiative recombination enhanced defect reactions in the active region due to the very low defect activation threshold typical for the wide bandgap II–VI's.

This paper presents a novel concept of the active region design for II–VI lasers, aimed at increase in their lifetime. The key points are (i) preventing the active region from outside penetration and development of extended and point defects and (ii) spatial separation of the radiative recombination and defect-containing sites in the active regions. The former problem is solved by incorporation of alternately-strained (Zn,Cd)Se/ZnSSe (or BeZnSe/ZnSe) short-period superlattice (SL) waveguide in the ZnMg(Be *or* S)Se/ZnCdSe separate confinement heterostructure (SCH) QW lasers, which results simultaneously in an improvement of the electronic and optical confinement. An exchange of the ordinary QW recombination region for a 2–3 monolayer (ML) thick CdSe fractional monolayer (FM) inserted in a ZnSe QW produces a satisfactory solution of the latter problem due to a transformation of CdSe FM under certain growth conditions into the array of self-organizing CdSe-rich nanoislands, which suppress dramatically the migration of non-equilibrium carriers to defects. It is expected also that using the Be chalcogenides with highest lattice rigidity among II–VI's contributes to raising the activation energy of defects formation and development [3].

2 Experiment

The (Zn,Mg)(S,Se)-based optically pumped laser structures were grown by molecular beam epitaxy (MBE) pseudomorphically on GaAs(001) substrates at a substrate temperature of 270–280°C for a study of properties of the novel active region itself. The (Be,Mg,Zn)Se-based laser diodes with the SL waveguide and different recombination regions were fabricated as well. The details of MBE growth and composition control of the S- and Be-containing laser structures have been published elsewhere [4, 5]. Besides the 0.5 μm-buffer and 0.1 μm-top $Zn_{0.92}Mg_{0.08}S_{0.15}Se_{0.85}$ layers, the optically pumped SL QW lasers include a 0.2 μm thick $ZnS_{0.14}Se_{0.86}$/(Zn, Cd)Se SL waveguide lattice-matched to GaAs as a whole and a single 7 nm-ZnCdSe QW in the middle. The CdSe mole fraction in the QW and SL has been varied from 0 to 0.27, which allows one to cover the lasing wavelength range from 470 to 523 nm. The active region of the CdSe FM laser structure contains 10 nm ZnSe QW as a matrix for a 2.8 ML CdSe insertion, surrounded by the 3 nm-$ZnS_{0.14}Se_{0.86}$/5 nm-ZnSe SL. The BeMgZnSe/ZnCdSe SCH laser diode structure contains a (1 nm-$Be_{0.05}Zn_{0.95}Se$/1.5 nm-ZnSe)$_{82}$ SL waveguide centered with either a 4 nm-$Zn_{0.63}Cd_{0.37}Se$ QW or a 10 nm-ZnSe QW incorporating the similar 2.6 ML CdSe FM sheet. The laser diode structure also involves 1 μm-thick wider-bandgap n- and p-$Be_{0.05}Mg_{0.06}Zn_{0.89}Se$ cladding layers, doped with iodine and nitrogen, respectively, as well as a ZnSe/BeTe:N modulation doped graded short-period SL capped with a highly p-doped BeTe:N/ZnTe:N contact structure. The details of MBE growth of the CdSe FM active region as well as the calibration procedure have been described elsewhere [6].

Transmission electron microscopy (TEM), including high resolution (HR) TEM, and x-ray diffraction (XRD) measurements were employed to characterize the laser structure parameters and structural quality. The cw and time resolved (20 ps) photoluminescence (PL) facilities were used for optical and transport studies. Lasing characteristics of the optically pumped lasers were studied using a N_2 laser with a 8 ns pulse width. The injection laser samples were fabricated by standard photolithography of stripe contacts and measured as described elsewhere [7].

3 Short-period alternately-strained superlattice waveguide

The general design, growth peculiarities and some properties of the alternately-strained II–VI SL and multiple QW (MQW) structures have been reported elsewhere [8, 9]. As

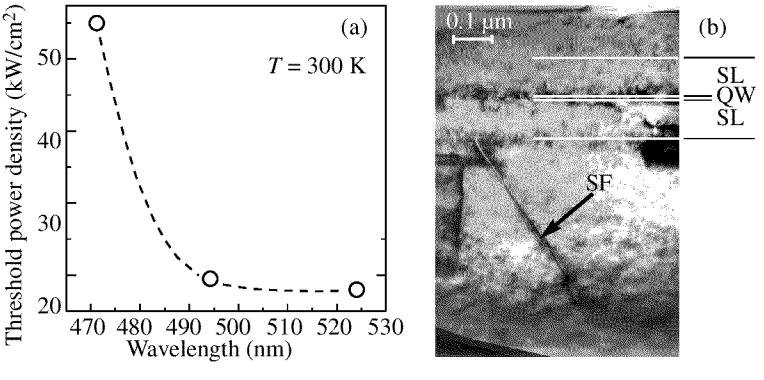

Fig. 1. (a) Room temperature threshold power density as a function of lasing wavelength for three SL QW laser structures with different compositions of (Zn,Cd)Se QW. (b) Cross-sectional TEM image of one of the structures, SF is a stacking fault.

has been shown in [8], the ZnSSe/ZnCdSe alternately-strained SLs and MQWs possess higher critical thickness's as compared to bulk layers with the same lattice mismatch and even exceed the theoretically estimated SL and MQW critical thickness's. The cross-sectional TEM image of the SCH SL QW structure, given in Fig. 1(b), demonstrates the great potential of the SL in protecting the laser active region from the extended defect (stacking fault) penetration. The threshold power density vs lasing wavelength is presented in Fig. 1(a) for three SL QW lasers demonstrating efficient room temperature (RT) operation ($P_{th} < 20\,kW/cm^2$) within a wide blue-green range (490–523 nm). These P_{th} values are among the lowest ever reported for optically pumped II–VI QW lasers, indicating improved electronic confinement for holes at the optimal optical confinement [10] as well as lowered concentration of non-radiative recombination centers in the QW.

Despite the lowest heavy-hole (*hh*) miniband in ZnSe-based SLs is rather narrow (typically $\sim$ 10 meV) due to the large effective mass ($0.6m_0$), extremely efficient carrier transport across the SLs has been observed by temperature-dependent cw and time-resolved (TR) PL measurements [11, 12]. Calculations of the band line-ups and confinement energies for a wide range of the ZnSSe/ZnCdSe SL structure parameters (thickness's and alloy compositions) show that the energy gap between the top of the lowest *hh* miniband, where exciton is essentially localized, and the bottom of the rather wide (30–100 meV) light-hole (*lh*) miniband does not exceed 10–15 meV. It provides efficient thermal occupation of the *lh* states with increasing temperature. This process appears to be responsible for the thermally-activated transfer of holes along the growth direction, followed by their capture into the QW and energy relaxation down to the lowest *hh* QW level.

The novel concept of the SL waveguide has been successfully realized in the RT BeMgZnSe/ZnCdSe SCH QW injection lasers by employing the BeZnSe/ZnSe alternately-strained SL surrounding deep ZnCdSe QW. The structures demonstrate a typical threshold current density of about $750\,A/cm^2$ (lowest value achieved is $\sim 450\,A/cm^2$) and threshold voltages around 7 V, which is mainly caused by still not completely optimized p-type doping of a cladding layer and optical confinement. The lasing spectra are presented in the inset of Fig. 2. However, some other parameters of the devices are not typical and are determined by the specific design of the active region. Figure 2 shows the temperature dependence of threshold current density of the SL QW laser diode with significantly enhanced characteristic temperature (up to $T_0 = 307$ K at RT), as compared to that of a conventional bulk-waveguide structure ($T_0 \sim 160$ K). This effect is associated namely with the improved electronic confinement of holes by the SL waveguide. For temperatures below 80 K, the threshold current has been found to decrease with increasing temperature, which is attributed to the thermally-activated carrier transport being even more efficient for the Be-contained SLs. In addition, a buried-ridge-waveguide laser diode with a 1 μm-stripe width yields T_0 as high as 360 K at and above RT, enabling pulsed laser operation up to 140°C [13]. These values are the highest ever reported for II–VI laser diodes.

4 CdSe/ZnSe fractional monolayer active region

It has recently been found that single CdSe/ZnSe FM structures exhibit bright excitonic PL, maximized in the vicinity of the CdSe critical thickness ($\sim$ 3 ML) ($\lambda \sim 520$ nm) [14]. The evolution of an intrinsic morphology and optical properties of single CdSe/ZnSe FM nanostructures and FM SLs within the CdSe nominal thickness range of 0.1–3.6 ML has been studied in detail by TEM, HR TEM, XRD, PL and TR PL in Refs. [6, 14–18]. A cross-sectional TEM image of the FM laser active region comprising both the SL waveguide and a single 2.8 ML CdSe FM recombination region is presented in Fig. 3(a). It demonstrates

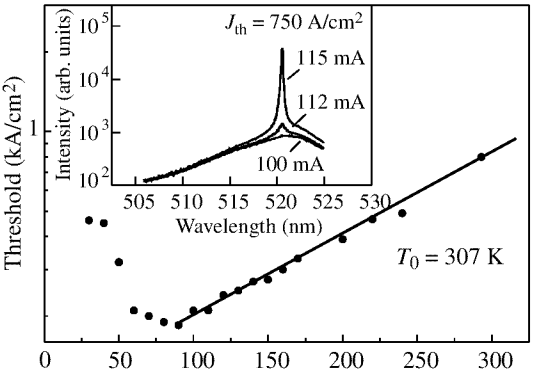

Fig. 2. Temperature dependence of threshold current density of BeMgZnSe SL QW laser diode. Inset shows its RT pulse lasing spectrum.

clearly visible elastic strain modulation of a thickness of the CdSe FM region, which can be attributed to the randomly distributed flat CdSe-enriched islands observed in the plan-view TEM picture (Fig. 3(b)). The plan-view TEM image shows the formation of 10–40 nm lateral size CdSe-based self-organized islands of about 2×10^{10} cm^{-2} density. Only $\sim$ 15% of the islands (the largest ones) look relaxed, whereas other 85% seem to be pseudomorphic. No extended defects are observed outside the large CdSe-based islands. The HR TEM study of single 2–3 ML CdSe/ZnSe FM structures revealed additionally a high density ($\sim 10^{11}$ cm^{-2}) of smaller CdSe-rich islands (8 $\pm$2 nm in lateral size), either separate or located within the larger islands as Cd composition fluctuations, which can contribute to the low energy PL tail of the structures. We believe that the dominant amount of deposited Cd is concentrated in the 2D-islands of ultra-thin QWs characterized by specific exciton localization potential due to Cd content fluctuations.

Lasing characteristics of the optically pumped ZnMgSSe laser with the CdSe FM active region are summarized in Fig. 3(c). The structure demonstrates about a 5-fold decrease in the RT threshold power density, down to $P_{th} = 3.9\,\mathrm{kW/cm^2}$ at $\lambda \sim 523$ nm, as compared

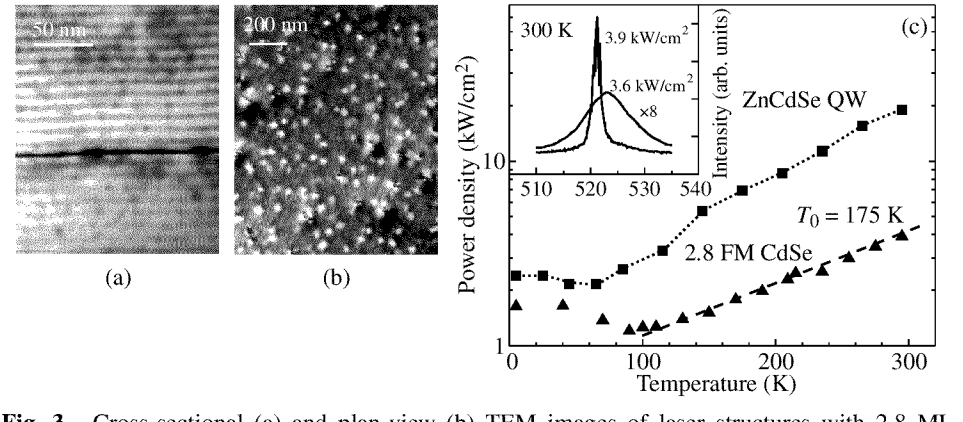

Fig. 3. Cross-sectional (a) and plan-view (b) TEM images of laser structures with 2.8 ML CdSe/ZnSe FM active region. (c) Temperature dependence of threshold power density for FM (triangle) and QW (square) laser structures. RT FM laser generation spectra are presented in the inset.

to the SL QW lasers operating at the same wavelength. The temperature dependences of threshold power density for both FM and QW laser structures are non-monotonic with noticeable minima at ~ 100 K and ~ 70 K, respectively, which can be attributed to different values of the *hh–lh* SL miniband gap governing the onset of the thermally-activated vertical carrier transport through the SLs. In addition, the FM laser does not show any noticeable degradation under the 25-fold threshold pumping power (~ 100 kW/cm^2) during 24 hours, whereas a conventional QW laser under the even more gentle conditions degrades completely within 1 hour. We speculate that the extremely low threshold of optically-pumped lasers and the enhanced degradation stability are related to the CdSe-based dot-like islands operating as efficient localization and recombination sites for the non-equilibrium carriers and preventing their migration to the larger relaxed islands and other defect regions, where they could decay non-radiatively, activating the defect development [19].

Figure 4(a) presents the cross-section TEM image of the BeMgZnSe laser diode active region comprising both the SL waveguide and the single 2.6 ML CdSe FM recombination region, which demonstrates the characteristic strain-field modulation of the FM region thickness. One should stress that the CdSe FM laser diode is the only among the series of RT SCH diodes, which has demonstrated a cw operation (see Fig. 4(b)), at all other equal conditions. Thus, first RT cw BeMgZnSe/(Zn)CdSe FM laser diodes have been fabricated.

5 Conclusions

In summary, we have presented a novel design of room-temperature ZnSe-based blue-green lasers using an alternately-strained SL waveguide, which demonstrate low (< 20 kW/cm^2) threshold power densities within the 470–523 nm range for optically pumped lasers and very high characteristic temperature (360 K at RT) due to the enhanced electronic confinement. The strained SL shows significantly increased stress stability and possibility of protecting the active region from the propagation of extended defects. In addition, the efficient mechanism of thermally-activated hole transport across the SL has been observed. Finally, employing a 2–3ML CdSe/ZnSe FM recombination region instead of a QW provides the lowest RT threshold power density ever reported for ZnSe-based lasers along with the enhanced degradation stability for both the optically and injection pumped lasers.

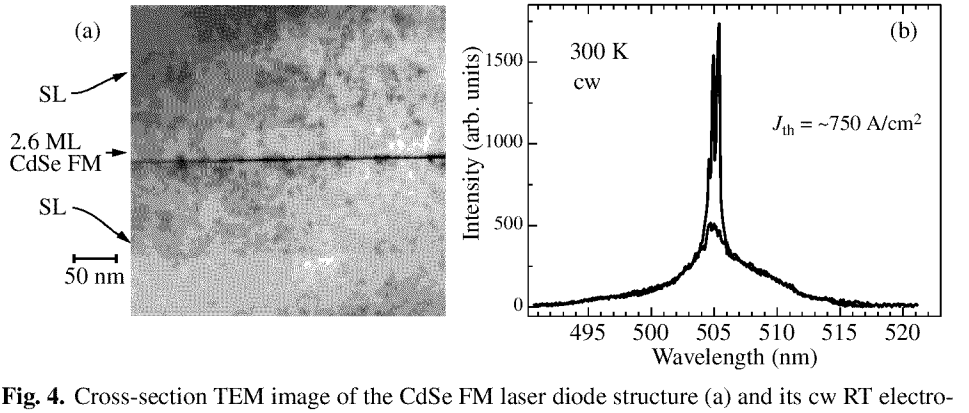

Fig. 4. Cross-section TEM image of the CdSe FM laser diode structure (a) and its cw RT electroluminescence spectra below and above threshold (b).

Acknowledgements

Authors appreciate greatly the technological and experimental collaboration with H.-J. Lugauer, G. Reusher, M. Keim, A. Waag and G. Landwehr (Universität Würzburg), G. R. Pozina, J. P. Bergman and B. Monemar (University of Linköping), N. Peranio, A. Rosenauer, D. Gerthsen (Universität Karlsruhe). Authors are thankful to A. A. Sitnikova for the TEM characterization of the structures, and N. D. Il'inskaya for the laser diode processing. This work has been supported in part by the RFBR grants, the Program of Ministry of Science of RF "Physics of solid-states nanostructures" as well as the Volkswagen-Stiftung.

References

[1] E. Kato, H. Noguchi, M. Nagai *et al.*, *Electron. Lett.* **34**, 282 (1998).
[2] K. Nakano, *Proc. 2nd Int. Symp. on Blue Laser and Light Emitting Diodes,* Chiba, 1998, p. 395.
[3] A. Waag, Th. Litz, F. Fischer *et al.*, *J. Cryst. Growth* **184/185**, 1 (1998).
[4] S. Ivanov, S. Sorokin, I. L. Krestnikov *et al.*, *J. Cryst. Growth* **184/185**, 70 (1998).
[5] A. Waag, F. Fischer, K. Schüll *et al.*, *Appl. Phys. Lett.* **70**, 1 (1997).
[6] S. V. Ivanov, A. A. Toropov, T. V. Shubina *et al.*, *J. Appl. Phys.* **83**, 3168 (1998).
[7] S. Ivanov, A. Toropov, S. Sorokin *et al.*, *Appl. Phys. Lett.* **73**, 2104 (1998).
[8] T. V. Shubina, S. V. Ivanov, A. A. Toropov *et al.*, *J. Cryst. Growth* **184/185**, 596 (1998).
[9] S. V. Ivanov, A. A. Toropov, S. V. Sorokin *et al.*, *Semicond.* **32**, 1137 (1998).
[10] A. A. Toropov, S. V. Ivanov, T. V. Shubina *et al.*, *Proc. Int. Symp. Nanostructures: Physics and Technology*, 1997 p. 210.
[11] A. Lebedev, S. Sorokin, A. Toropov *et al.*, *Acta Physica Polonica A* **94** (2), 421 (1998).
[12] A. Toropov, T. V. Shubina, A. V. Lebedev *et al.*, *Proc. 2nd Int. Symp. Blue Laser and Light Emitting Diodes*, Eds. K.Onabe *et al.*, (1998, Chiba, Japan), p. 254.
[13] M. Legge, S. Bader, G. Bacher *et al.*, *ibid*, p. 409.
[14] A. A. Toropov, S. V. Ivanov, T. V. Shubina *et al.*, *Jpn. J. Appl. Phys.* **38**, 566 (1999).
[15] A. A. Toropov, S. V. Ivanov, T. V. Shubina *et al.*, *J. Cryst. Growth* **184/185**, 293 (1998).
[16] I. Sedova, T. Shubina, S. Sorokin *et al.*, *Acta Physica Polonica A* **94** (3), 519 (1998).
[17] A. A. Toropov, T. V. Shubina, S. V. Sorokin *et al.*, *Phys. Rev. B* **59**, 2510 (1999).
[18] N. Peranio, A. Rosenauer, D. Gerthsen *et al.*, *Submitted to Phys. Rev. Lett.* (1999).
[19] S. V. Ivanov, A. A. Toropov, S. V. Sorokin *et al.*, *Appl. Phys. Lett.* **74**, 498 (1999).